Fracture mechanics properties of Al/Steel Structural Transition Joints for shipbuilding

Pasqualino CORIGLIANO[a,1] , Vincenzo CRUPI and Pingsha DONG[b]
[a] *Department of Engineering, University of Messina, Contrada Di Dio (S. Agata), 98166 Messina, Italy: pcorigliano@unime.it, crupi.vincenzo@unime.it*
[b] *Department of Naval Architecture and Marine Engineering, University of Michigan, Ann Arbor, MI 48105, United States: dongp@umich.edu.*

Abstract. The need of lowering the weight of ships makes it crucial to have superstructures made of aluminum alloy and the ship hull made of steel. Within this context, the connection between the two different metals becomes crucial as different metals are hardly weldable using traditional techniques. Thus Structural Transition Joints are extremely important. One of the most promising welding techniques is the Explosion Welding process, which reaches a good compromise between weldability and mechanical properties of Structural Transition Joints. In the present study, the mechanical behaviour of Structural Transition Joints made of ASTM A516 structural steel, clad by explosion welding with AA5086 aluminum alloy and provided with an intermediate layer of pure aluminum was investigated. Preliminary fracture mechanics tests on CT Specimens made of Al alloy and shipbuilding grade steel were performed. Afterwards, fracture mechanics properties of the Structural Transition Joint considering a notch located at the interface between the pure aluminum and steel were evaluated experimentally following the current standards. In addition, the Digital Image Correlation technique allowed the analysis of the displacement and strain patterns of the different metals and to evaluate the crack length of the bimetallic specimen.

Keywords. Explosive Welded joints, Ship structures, Digital Image Correlation, Fracture mechanics.

1. Introduction

The shipbuilding and offshore structures involve several metallic materials, ranging from standard steel to high strength steels, passing by aluminium and titanium alloys. Undoubtedly the main connection technique is represented by welding, but the problem of joining different materials still represents an important challenge.
In the recent years, the explosion welding (EW) technique [1] has been increasingly applied for joining dissimilar metallic materials instead of the conventional welding techniques, due to likely technical complications such as metallurgical incompatibility. The EW is usually described as a solid-state joining process. This process uses an explosive detonation as the energy source to produce a metallurgical bond between metal components. This produces partial melting at the wavy interface and the growth of intermetallics, that can be the source of cracking when exposed to dynamic loading.

[1] Corresponding Author. Pasqualino Corigliano, University of Messina, Department of Engineering, Contrada Di Dio (S. Agata), 98166 Messina, Italy; E-mail: pcorigliano@unime.it.

The most used Structural Transition Joints (STJ) in shipbuilding industries are Al/Steel joints [1–5], while Ti/Inconel [6] and Stainless steel/Inconel 625 [7] joints are principally employed for offshore and oil & gas industry. A case of steel hull to Al superstructure connection is shown in Figure 1, where dissimilar Al/Steel STJ were used between the yacht's hull and superstructure [8, 9] in order to weld by means of traditional welding techniques the steel hull side on the to the steel side and the aluminium upper section to the Al side of the bimetallic joint.

Figure 1. Welding steel hull to aluminium superstructure [8].

Another shipbuilding application of bimetallic joints for the connection of aluminium superstructure to steel deck is reported in [10].

Some investigations on Al/Steel STJs are reported in literature: static and fatigue bending tests [3], non linear finite element simulations of bending tests [5], tensile-shear and Charpy Impact tests [4], hardness measurements and static tensile tests [11], fracture mechanics tests [12]. The interfacial toughness of a shipboard Al/Steel STJ was investigated in [12], applying bending tests, and it was found that the interfacial toughness increases as the mode II (shearing mode) increases. The ship structures are exposed to severe seas and long-term wave loads, so the random sea states effect on the fatigue life of Al/Steel STJ, estimated by means the frequency domain method, was investigated in [13].

Up to the authors knowledge, the fracture mechanics and the crack propagation analyses for Al/Steel STJ are not sufficiently discussed in literature. The aim of this study was to assess the linear elastic fracture mechanics (LEFM) properties and to monitor the crack propagation in Al/Steel STJ according to the ASTM standards [14, 15]. Preliminary, the LEFM tests were performed on Compact Tension (CT) specimens, made of the base materials, in order to compare the results with the ones obtained on CT specimens, made of Al/Steel STJ. The crack length of the STJ was monitored considering the discontinuity point of the displacement field in the loading direction [16] by means of the Digital Image Correlation (DIC), which was already applied by the authors to different kinds of joints [5, 17–19] . A DIC-based structural strain approach for low-cycle fatigue assessment of welded joints was recently developed by the authors [17]. More information about the DIC system used can be found in [17].

2. Fracture mechanics properties of the base material specimens

The geometry of the CT specimens was chosen according to ASTM E399 [14], as shown in Figure 2 for the two base materials: ASTM A516 Gr.55 steel and 5086 aluminum alloy, which are typically used for ship structures. The ASTM E399 standards involve plane strain specimen geometries, if thinner specimens are investigated, the LEFM formulae should be corrected properly accounting for plane stress conditions.

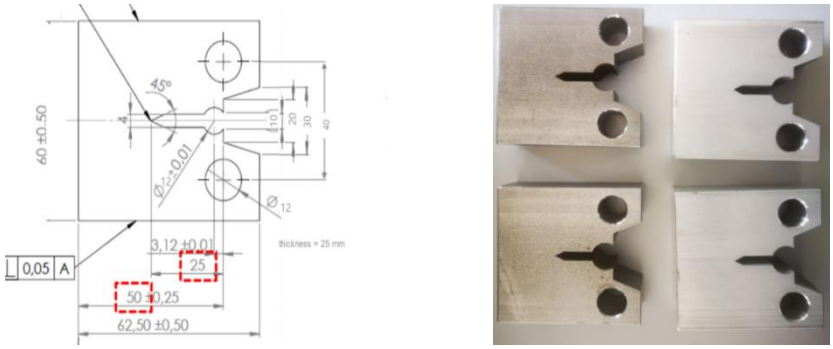

a) b)

Figure 2. Geometry according to ASTM E399 (a) and CT specimens (b).

Preliminary some cyclic tests were carried out to complete fracture, in order to obtain the three phases (crack initiation, stable crack propagation, unstable crack propagation) and the Paris curves, each of the two investigated materials. The crack length during the crack propagation tests was calculated by means of the compliance method according to the ASTM E 647 standard [15].

The interpolation of the experimental data in the phase of the stable crack propagation, allowed to derive the Paris law, shown in Figure 3.

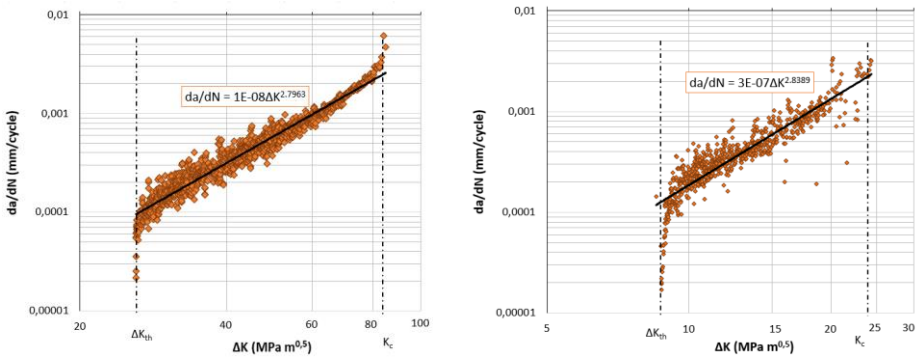

a) b)

Figure 3. Paris curve for steel (a) and aluminium alloy (b) CT specimens.

Subsequently, LEFM tests were performed according to ASTM E399 [14], following two phases:

1. pre-cracking of the CT specimens due to fatigue loadings according to the ASTM E 647 standard [15], until a predetermined value of the length of the crack, set equal

to 30 mm, is reached in order to have a very sharp notch and to ensure that the crack propagation is perpendicular to the loading direction;

2. destructive test of the CT specimens, by constantly increasing the tensile stress, during which the load and the crack opening displacement (C.O.D.), correlated to the crack propagation, is recorded by means of a clip gage.

Figure 4 shows the trend of the load as a function of the displacement determined by the crack opening during the second phase of the LEFM tests.

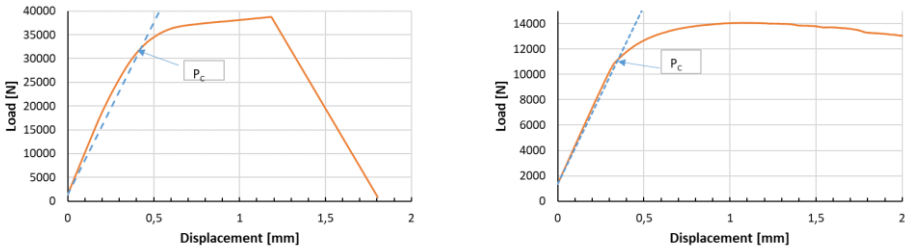

a) b)

Figure 4. Loading- displacement curves steel (a) and aluminium alloy (b) CT specimens.

The stress intensification factor K_{IC} was derived according to the following procedure [19]:

- the tangent line to the initial linear section of the curve shown in Figure 4;
- the straight line having a slope equal to 95% of the previous one has been identified;
- the intersection between this straight line and the load-displacement curve allows to evaluate the values of P_C load level (P_C = 32.13 kN for steel, P_C =11.09 kN for aluminium alloy).
- the crack length *a*, given by the sum of the length of the carving and the crack propagation in the first phase of the tests, has been measured at the two external surfaces and at 25%, 50% and 75% of the specimen thickness;
- the corrective factor *f(a/W)* has been evaluated, according to ASTM E399;
- finally, the value of K_{IC} was calculated, according to the following equations

$$K_{Ic} = \frac{P_c}{\sqrt{B\sqrt{W}}} f\left(\frac{a}{W}\right) \quad (1)$$

The K_{IC} and ΔK_{th} values evaluated for both materials are given in Table 1.

Table 1. Experimental values of K_{IC} and ΔK_{th}.

Material	**K_{IC}** [MPa $m^{0.5}$]	**ΔK_{th}** [MPa $m^{0.5}$]
ASTM A516 Gr.55 steel	74.20	26.05
5086 Aluminum alloy	25.65	8.75

The K_{IC} is difficult to measure since it requires plane-strain conditions, still the specimen geometry was chosen according to the ASTM E399 standard [14] to achieve this condition. The values of K_{IC} may be slightly queationable for both metals, due to plane-strain conditions and plastic deformation shown in Figure 4, even if the K_{IC} value evaluated for the AA 5086 alloy is similar to the one (27 MPa $\circ$ $m^{0.5}$) reported in the ASM handbook [20]. CTOD measurements will be performed in future studies. However, the results of the present research activity give a qualitative comparison between the two base materials, and they will be refined in future studies to take into account plastic deformation.

3. Stress Intensity Factor of the STJ and crack tip monitoring by means of the DIC technique

The bimetallic bars were supplied by the Nobleclad company and are made of ASTM A516 Gr.55 steel / Aluminum 1050A / 5086 Aluminum alloy. The geometry of the CT specimens with thickness t = 10 mm are shown in Figure 5. The STJ specimens have three layers with different heights: 19 mm for ASTM A516 Gr.55 steel, 9.5 mm for the intermediate layer of AA1050 aluminum, 6 mm for AA5086 aluminum alloy.

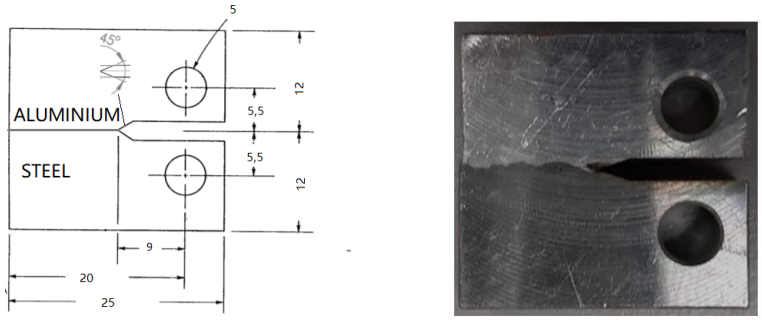

a b

Figure 5. Geometry according to ASTM E399 (a) and b) CT specimens (b).

The LEFM tests were performed, according to ASTM E399 [14], on the STJ specimens. These specimens were manufactured by means of electrical discharge machining (EDM) in order to obtain the crack propagation tip at the steel/aluminum interface and a crack mouth of 2 mm. Since no clip gage was available for such a low measure of the crack mouth, the DIC technique was used to determine the crack length during its propagation. Thus, a method for detecting the crack position by means of the DIC was setup. It must be said that, due to the wavy interface between steel and aluminium, the manufacturing of the notch did not always occur at the interface, but the crack initiation and propagation occurred always at the bimetallic interface as experimentally observed. In addition, due to the presence of the interface, no fatigue pre-cracking was needed as the crack naturally propagates across the interface between steel and aluminium. The load-displacement curve obtained during the LEFM tests is shown in Figure 6.

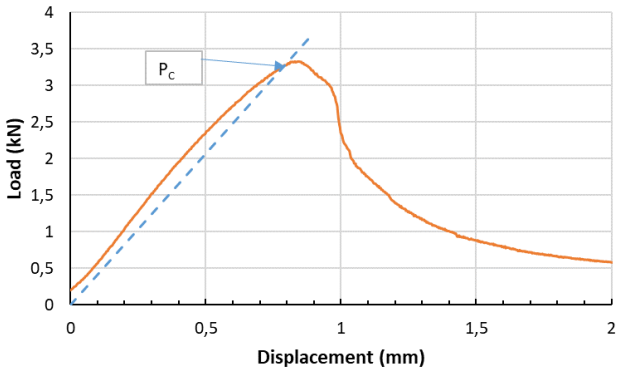

Figure 6. Loading- displacement curve for K evaluation in STJ specimen.

The critical stress intensity factor K_{Ic} was evaluated as already described for the CT specimens, made of steel and aluminium alloy. The obtained results, calculated according to [14], are shown in Table 2. It is worth to be mentioned that the K_{IC} value, obtained for STJ, is about 20 % lower than that of the aluminium alloy reported in Table 1.

Table 2. LEFM parameters of the investigated STJ. Parameters defined in [14].

P_C [kN]	a [cm]	B [cm]	w [cm]	f(a/w)	K_{IC} [MPa $m^{0.5}$]
3.25	0,9	1	2	8.34	19.16

Considering that an intermediate layer of pure Al is placed between the Al alloy and the structural steel, the obtained value looks satisfactory. The failure surface resulted wavy following the morphology of the Al/Steel interface, as shown in Figure 7.

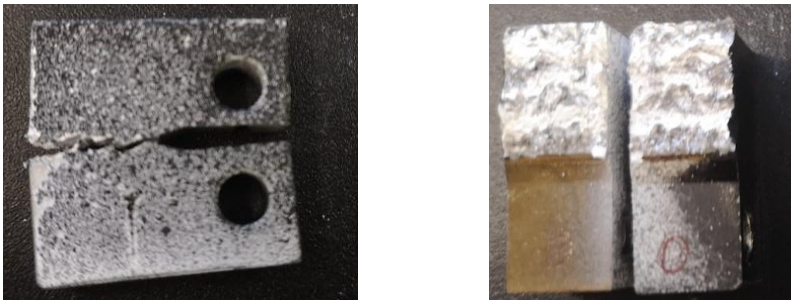

Figure 7. Fractured specimen.

The wavy interface plays an important role for the K_{Ic} value as it makes the crack deviate from a fully horizontal path and follows the wavy morphology of the interface. This means that there is a Mode II effect, thus the K_{II} should be evaluated in future studies.

In order to setup a method for detecting the crack length, that should be used especially during fatigue loading to determine the Paris law, the vertical displacement distribution was determined by means of the DIC method.

The analysis of the displacement distribution in the loading direction allowed the identification of the displacement discontinuity. This can be interpreted as a material discontinuity caused by the fatigue crack. Thus, by analyzing the displacement gradient, the current position of the crack can be identified. The displacement distribution during the test is reported in Figures 8. The images clearly show the displacement is uniform in the first phase of the test (a), while a discontinuity is observed at max load (b), indicating that the crack length changed. The right side of Figure 8 reports the magnification of the strain near the crack tip. This behaviour is confirmed in Figure 9, where three points at a distance of 0,5 mm from the crack tip are analyzed. The curves of the three points are overlapped the same values, while the lower point follows a different displacement trend when the crack occurs after 30 s.

Moreover the DIC technique allowed the evaluation of von Mises strain, as reported in Figure 10 at 2 kN and at max load, showing the high level of strain.

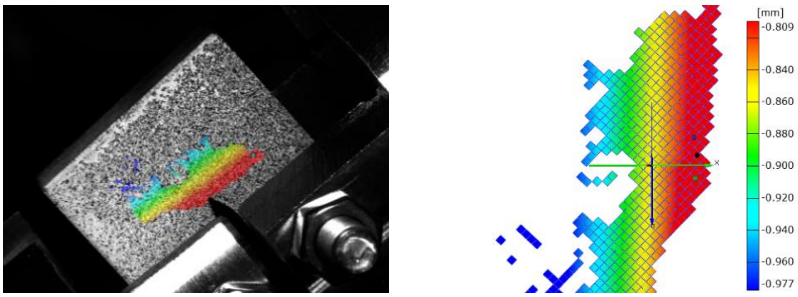

(a) prior to maximum loading (3.25 kN)

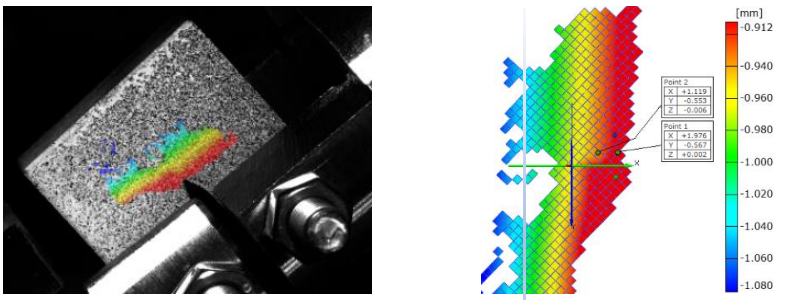

(b) crack initiation at maximum loading (3.33 kN)

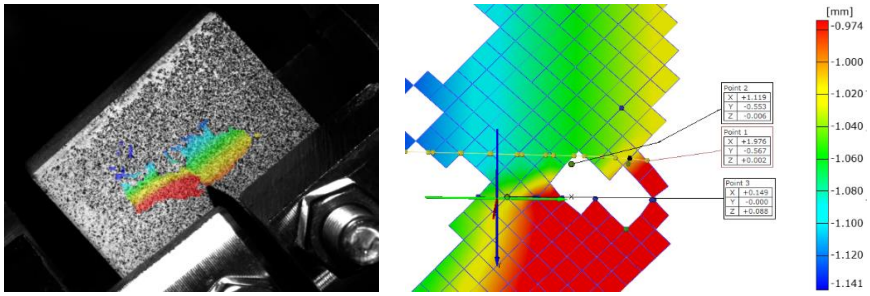

(c) crack propagation after maximum loading (3.25 kN)

Figure 8. Displacement distribution around the crack tip

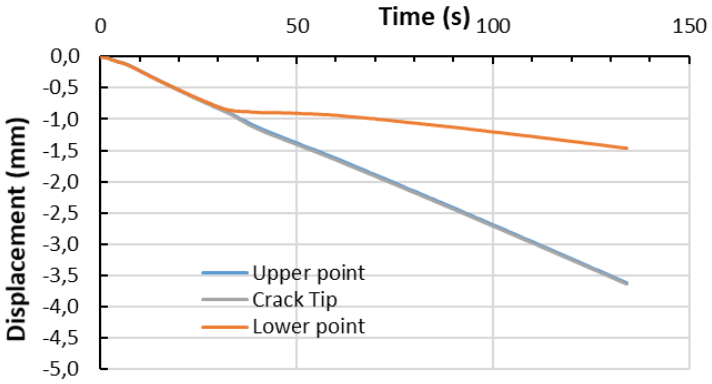

Figure 9. Displacement evolution of three points near the crack tip.

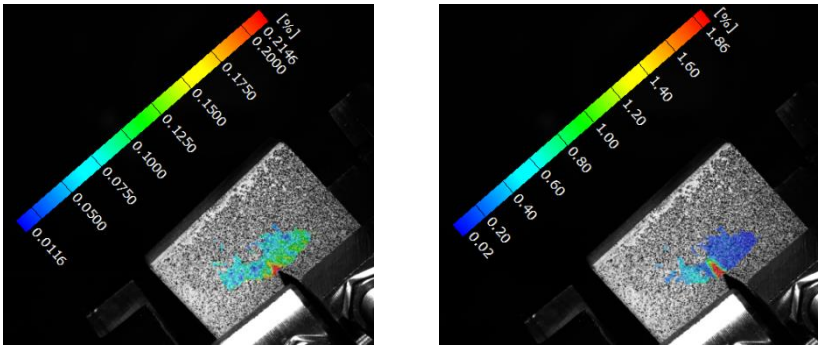

(a) (b)

Figure 10. Von Mises strain at 2 kN (a) and max load (b).

Conclusions

The crack length on steel and aluminium alloy CT specimens was calculated during crack propagations tests by means of the compliance method according to the ASTM E 647 standard.

The interpolation of the experimental data in the stable crack propagation phase of the crack, allowed to derive the Paris law. The LEFM tests according to ASTM E399 standard allowed to evaluate the mode I Stress Intensity Factor.

The Al/Steel STJ were also investigated and CT specimens were manufactured by EDM placing the crack tip in correspondence of the Al/Steel wavy interface. The tests allowed the determination of the mode I Stress Intensity Factor according to ASTM E399 standard. The wavy interface plays an important role for the K_{Ic} and the obtained value resulted satisfactory. However, the Mode II effects need to be considered in performing both DIC and load-CMOD curve analysis, which will be addressed in future studies.

In addition, the failure surface resulted wavy, following the morphology of the Al/Steel interface. The DIC was used to setup a method of measuring the crack length of

the STJ. In addition, the DIC technique was used to evaluate the von Mises strain during the test.

A DIC- based technique will be set up to measure the crack length propagation during fatigue testing of STJ CT specimens for obtaining the Paris law also for the STJ in future studies.

Acknowledgements

The experiments reported in this scientific activity were conducted with the support of Research Project "THALASSA", funded by the PON (National Operative Programme) 2014-2020.

Reference

[1] Findik F. Recent developments in explosive welding [Internet]. Vol. 32, Materials and Design. 2011 [cited 2017 Mar 15]. p. 1081–93. Available from: http://linkinghub.elsevier.com/retrieve/pii/S0261306910006138

[2] Ayob F. JOINING OF DISSIMILAR MATERIALS BY DIFFUSION BONDING/ DIFFUSION WELDING FOR SHIP APPLICATION [Internet]. Vol. 1, Marine Frontier. 2010 [cited 2021 Jan 9]. Available from: http://www.mimet.edu.my/v07/images/stories/marinefrontier/marine_frontier_vol2_2010_ver2.pdf#page=70

[3] Corigliano P, Crupi V, Guglielmino E, Mariano Sili A. Full-field analysis of AL/FE explosive welded joints for shipbuilding applications. Mar Struct. 2018;57:207–18.

[4] Kaya Y. Microstructural, Mechanical and Corrosion Investigations of Ship Steel-Aluminum Bimetal Composites Produced by Explosive Welding. Metals (Basel) [Internet]. 2018 Jul 15 [cited 2020 Sep 11];8(7):544. Available from: http://www.mdpi.com/2075-4701/8/7/544

[5] Corigliano P, Crupi V, Guglielmino E. Non linear finite element simulation of explosive welded joints of dissimilar metals for shipbuilding applications. Ocean Eng. 2018;160:346–53.

[6] Corigliano P, Crupi V. Fatigue analysis of TI6AL4V / INCONEL 625 dissimilar welded joints. Ocean Eng [Internet]. 2021;221(January):108582. Available from: https://doi.org/10.1016/j.oceaneng.2021.108582

[7] Milititsky M, Gittos FM, Smith SE, Marques V. Dissimilar Metals for Sub-Sea use under Cathodic Protection - TWI. In: Materials Science & Technology 2010. Houston, Texas U, editor. 2010 [cited 2020 Sep 10]. Available from: https://www.twi-global.com/technical-knowledge/published-papers/assessment-of-dissimilar-metal-interfaces-for-sub-sea-application-under-cathodic-protection

[8] 70m Benetti Superyacht FB273 Launched - Luxury Projects [Internet]. [cited 2022 Feb 26]. Available from: https://www.luxury-projects.it/70m-benetti-superyacht-fb273-launched/

[9] BENETTI 65-METER CUSTOM YACHT FB274 TAKES SHAPE. HULL AND SUPERSTRUCTURE JOINED TOGETHER | Benetti Yachts [Internet]. [cited 2022 Feb 26]. Available from: https://www.benettiyachts.it/news-

events/benetti-65-meter-custom-yacht-fb274-takes-shape-hull-and-superstructure-joined-together/
[10] Young GA, Banker JG. Explosion welded, BI-metallic solutions to dissimilar metal joining. In: SNAME 13th Offshore Symposium [Internet]. 2004 [cited 2022 Mar 19]. p. 149–54. Available from: https://onepetro.org/SNAMETOS/proceedings-abstract/TOS0413/1-TOS0413/D013S005R002/181606
[11] Borońśki D, Skibicki A, Maćkowiak P, Płaczek D. Modeling and analysis of thin-walled Al/steel explosion welded transition joints for shipbuilding applications. Mar Struct. 2020 Nov 1;74:102843.
[12] Chao RM, Yang JM, Lay SR. Interfacial toughness for the shipboard aluminum/steel structural transition joint. Mar Struct. 1997;10(5):353–62.
[13] Böhm M, Kowalski M. Fatigue life estimation of explosive cladded transition joints with the use of the spectral method for the case of a random sea state. Mar Struct. 2020 May 1;71:102739.
[14] Standard Test Method for Linear-Elastic Plane-Strain Fracture Toughness of Metallic Materials [Internet]. [cited 2022 Mar 26]. Available from: https://www.astm.org/standards/e399
[15] Standard Test Method for Measurement of Fatigue Crack Growth Rates [Internet]. [cited 2022 Mar 26]. Available from: https://www.astm.org/standards/e647
[16] Sołtysiak R, Borońśki D, Kotyk M. Experimental verification of the crack opening displacement using finite element method for CT specimens made of Ti6Al4V titanium alloy. AIP Conf Proc [Internet]. 2016 Oct 20 [cited 2022 Mar 26];1780(1):050006. Available from: https://aip.scitation.org/doi/abs/10.1063/1.4965953
[17] Corigliano P, Crupi V, Pei X, Dong P. DIC-based structural strain approach for low-cycle fatigue assessment of AA 5083 welded joints. Theor Appl Fract Mech [Internet]. 2021 Dec 1 [cited 2021 Oct 3];116:103090. Available from: https://linkinghub.elsevier.com/retrieve/pii/S0167844221001944
[18] Corigliano P. On the Compression Instability during Static and Low-Cycle Fatigue Loadings of AA 5083 Welded Joints: Full-Field and Numerical Analyses. J Mar Sci Eng [Internet]. 2022 Feb 5 [cited 2022 Feb 20];10(2):212. Available from: https://www.mdpi.com/2077-1312/10/2/212/htm
[19] Corigliano P, Ragni M, Castagnetti D, Crupi V, Guglielmino E. Measuring the static shear strength of anaerobic adhesives in finite thickness under high pressure. J Adhes. 2021;97(8):783–800.
[20] Lampman SR. ASM Handbook: Volume 19, Fatigue and Fracture. Vol. 19, ASM International. 1996. 557–565 p.